Atmospheric blocking: space-time links to the NAO and PNA

Mischa Croci-Maspoli · Cornelia Schwierz ·
Huw C. Davies

Abstract In the Northern hemisphere, regions characterized by an enhanced frequency of atmospheric blocking overlap significantly with those associated with the major extra-tropical patterns of large-scale climate variability—namely the North Atlantic Oscillation (NAO) and the Pacific North American (PNA) pattern. There is likewise an overlap in the temporal band-width of blocks and these climate patterns. Here the nature of the linkage between blocks and the climate patterns is explored by using the ERA-40 re-analysis data set to examine (1) their temporal and spatial correlation and (2) the interrelationship between blocks and the NAO/PNA. It is shown that a strong anti-correlation exists between blocking occurrence and the phase of the NAO (PNA) in the North Atlantic (western North Pacific), and that there are distinctive inter-basin differences with a clear geographical (over North Atlantic) and quantitative (over North Pacific) separation of typical blocking genesis/lysis regions during the opposing phases of the climate patterns. An Empirical Orthogonal Function (EOF) analysis points to a significant influence of blocking upon the NAO pattern (identifiable as the leading EOF in the Euro-Atlantic), and a temporal analysis indicates that long-lasting blocks are associated with the development of negative NAO/PNA index values throughout their life-time. In addition an indication of a cause-and effect relationship is set-out for the North Atlantic linkage.

M. Croci-Maspoli (✉) · C. Schwierz · H. C. Davies
Institute for Atmospheric and Climate Science,
ETH Zurich, CHN M16.3, 8092 Zurich, Switzerland
e-mail: mischa@env.ethz.ch

1 Introduction

The identification of individual blocking events in climatological data sets using various objective blocking indices shows a general consistency in the spatial distribution of blocks and their temporal duration (e.g. Dole and Gordon 1983; Tibaldi and Molteni 1990; Lupo and Smith 1995; Sausen et al. 1995; Pelly and Hoskins 2003; Croci-Maspoli et al. 2007). Namely the overall geographical distribution shows a bimodal frequency structure with maximum blocking frequency along the storm track regions of both the North Atlantic and Pacific basins. The temporal duration of individual blocking events is not always explicitly defined in the literature, but minimum life-times have been proposed in the range from 3 to 10 days. However, an entire blocking life-cycle can be of the order of several days up to weeks.

The predilection for blocking occurrence in the two ocean basins and the relatively long blocking life-times prompt consideration of a link between atmospheric blocking and the dominant large-scale patterns of inter-annual/seasonal climate variability in the Northern Hemisphere. The patterns considered in this study are the North Atlantic Oscillation (NAO) and the Pacific North American (PNA) pattern, and these contribute most to the winter atmospheric variability in the corresponding regions (Wallace and Gutzler 1981).

Several studies have examined the statistical relation between atmospheric blocking and respectively the NAO (e.g. Pavan and Doblas-Reyes 2000; Stein 2000; Shabbar et al. 2001; Scherrer et al. 2006) and the PNA (e.g. Renwick and Wallace 1996; Huang et al. 2002). However, our understanding of the dynamical mechanisms linking blocking and NAO/PNA remains meagre. A dynamically based study analysing blocking and the NAO (Shabbar

et al. 2001) suggests that the surface temperature contrast between land and sea favours the formation and persistence of blocks. The accompanying statistical correlation between blocking and the NAO for the Euro-Atlantic sector revealed a significantly increased blocking frequency during the negative NAO phase over the western North Atlantic ocean. These findings are corroborated in the recent study of Scherrer et al. (2006) who applied three different two-dimensional blocking indices. In addition they point to significant positive correlations between blocks and the NAO over the western European continent. A recent statistically based study (Barriopedro et al. 2006) confirms the latter findings for the Euro-Atlantic sector.

Similar studies for the North Pacific basin but now considering the 'block-PNA' linkage reveals a sensitivity of blocking occurrence in the Bering Strait to the polarity of the PNA (Renwick and Wallace 1996). However, this study indicates that blocking in this region is even more sensitive to the ENSO cycle, and this linkage is also highlighted in other studies (e.g. Straus and Shukla 2002). Another study (Huang et al. 2002) links winters with strong blocking in the North Pacific to the geopotential height anomalies akin to a PNA-like pattern.

This recent spate of studies of the ''block-climate pattern' linkage focussed primarily on statistical correlation, as opposed to the physical linkage between blocks and the dominant patterns of climate variability. This emphasis is attributable in part to the nature of the indicators deployed to detect blocks (predominantly quasi-one-dimensional indices) that hamper direct dynamical analyses. However, the studies do prompt questions related to the intrinsic nature of blocks, and in particular the issue of how and to what extent do blocks influence the variability patterns or vice versa. Dynamical considerations of the establishment of the NAO (Feldstein 2003; Benedict et al. 2004) and PNA (Feldstein 2002), stress on the one hand the importance of nonlinear processes for the NAO life-cycle and on the other hand the primacy of linear processes for the PNA evolution. In addition they point to the importance of synoptic-scale waves that either break cyclonically (negative NAO) or anti-cyclonically (positive NAO) for the establishment of the opposing NAO phases. Noting that wave breaking can also influence blocking formation, it can be argued that a block's life-cycle can also play an integral role in the establishment and temporal variation of the NAO/PNA.

This study's goals are twofold. First an attempt is made to derive a refined description of the temporal and spatial correlations between atmospheric blocking and the dominant climate modes. To this end a two-dimensional blocking index (Schwierz et al. 2004) is applied that identifies in a dynamically consistent fashion a block's location, spatial extent, movement and its genesis and lysis location. Second novel insight is sought on the temporal relationship between atmospheric blocking and the dominant modes of variability including consideration of whether atmospheric blockings alter the phase of the NAO and PNA in respectively the North Atlantic and North Pacific basin.

The study is structured as follows. In Section 2 the data and methodology is set out that are used to analyse blocking and the NAO/PNA patterns. Section 3 provides separate composite analyses for the Euro-Atlantic (NAO) and North Pacific (PNA) regions. In Section 4 an Empirical Orthogonal Function (EOF) analyses is applied to two different data sets to examine the importance of the blocks in the establishment of climate modes, and in Section 5 a more dynamical interpretation is provided of the nature of the linkage between blocking and the NAO and PNA. Finally in Section 6 the study's main findings are listed and critically reviewed.

2 Data and methodology

In this study the Northern Hemispheric ERA-40 re-analysis (Uppala et al. 2005) data from the European Centre for Medium Weather Forecast (ECMWF) is used for the boreal winter time periods Dec. 1957 to Feb. 2002 (DJF). The temporal resolution is 6 h (00, 06, 12, 18 UTC) and the T159L60 spectral model data is interpolated horizontally on a $1° × 1°$ grid. The hydrostatic form of the Ertel potential vorticity (PV) (Ertel 1942) provides the key analysis parameter for blocking detection. Atmospheric blocking episodes are calculated using the PV-based blocking index defined by Schwierz et al. (2004) which identifies vertically coherent negative (for the Northern Hemisphere) PV anomalies at tropopause altitudes. Their APV* index is calculated first by computing the Vertically Averaged PV (VAPV) between 500 and 150 hPa. The two pressure boundaries are chosen so that they encompass the entire tropopause region and the core PV anomaly of the block. Second, a tracking algorithm identifies the negative PV anomalies (relative to the long-term climatology) that persist for longer than 5 days. These are then regarded as atmospheric blocks. The tracking makes use of an overlap criterion (70%) of two consecutive negative PV anomalies, and the centre of the block is defined as the centre of mass of the negative PV anomaly. This procedure provides detailed information about the entire blocking life-cycle including the exact geographical location, the spatial scale and the intensity. Furthermore, blocking genesis/lysis is defined as the time step of the first/last blocking detection of the tracking procedure. An illustrative example of a typical blocking

Fig. 1 Comparison between the regional monthly mean APV* blocking frequency (*dark shading*) in (**a**) the West Atlantic (55°–65°N, 70°–50°W) and **b** the East Pacific (45°–55°N, 160°–180°W) and the corresponding monthly NAO/PNA index (*light shading*). The distributions are standardized in a way such that the maximum blocking frequency and the minimum NAO/PNA index within the entire time period attain a maximum value of 1 and –1, respectively
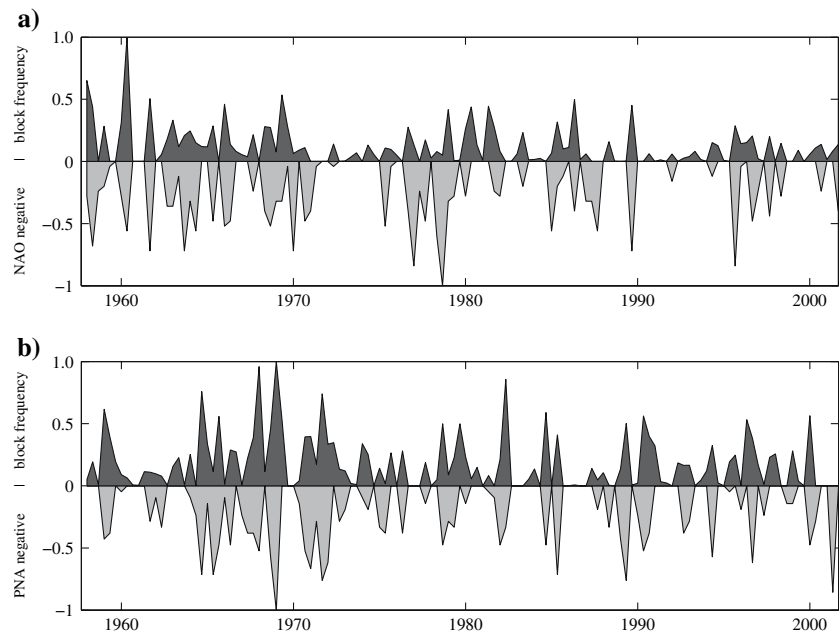
life-cycle can be found in Fig. 1 of Croci-Maspoli et al. (2007). It is to be noted that, in comparison to the results derived using quasi-one-dimensional blocking indices, the present technique of tracking individual blocks allows more dynamically based investigations.

For the composite analysis the potential temperature distribution on the 2 pvu (1 pvu = 10^{-6} K kg^{-1} m^2 s^{-1}) iso-surface (PV2) is used. In addition the geopotential height at 500 hPa (Z500) is used to apply an EOF analysis on a monthly basis. Only the first three winter EOFs are considered in this study and are displayed as geographical deviations from the climatological Z500 winter mean. Herein the EOFs are based on the covariance-matrix and the data is cosine-latitude weighted and de-trended before application. Also recall that the corresponding Principal Components (PC) give an indication of the temporal evolution of the individual EOF patterns.

For the detection of anomalous NAO/PNA index phases the daily indices from the Climate Prediction Center (CPC) are adopted for the same fore-mentioned winter period. It must be mentioned here that the procedure of calculating the daily indices has been adjusted by the CPC in 2005. A brief comparison between the previous and current daily indices shows some discrepancies in the magnitude of the standardized indices, but the phase transitions are reasonably consistent between these two indices (not shown). In this study, the earlier index time-series has been used. The NAO/PNA indices have been standardized by one standard deviation and divided into three terciles (positive = +, neutral = $_n$ and negative = –). The following tercile values for the winter index series emerge: NAO+ > 0.52, NAO– < –0.34, PNA+ > 0.52 and PNA– < –0.39.

3 Temporal and spatial correlations

It was noted earlier that most of the recent studies examining the correlation between atmospheric blocking and the patterns of variability have focussed on the temporal correlation. However, the spatial blocking distribution is also crucial for analysing the space-time correlation. Therefore, here, both the temporal and spatial resolution are analysed for the NAO and PNA separately.

3.1 Motivation

Figure 1 provides striking evidence for the temporal correlation between the occurrence of atmospheric blocking and the negative phase of the NAO/PNA. An index of the regional mean blocking frequency (Croci-Maspoli et al. 2007) is displayed on a winter monthly basis for the period between 1958 and 2002 against the series of the negative NAO/PNA index. For both regions the blocking frequency and the NAO/PNA indices are standardized in a way such that the maximum blocking frequency and the minimum NAO/PNA index within the entire time period attain a maximum value of 1 and –1, respectively. The evident temporal correlation between the enhanced blocking occurrence and the negative NAO/PNA phases suggests a strong linkage between atmospheric blocking and both pattern indices [both are statistically significant at the 95%-level using linear rank correlations with (a) $R = 0.5$ and (b) $R = 0.62$]. In effect winter months with negative NAO/PNA index values tend to have enhanced blocking frequency and vice versa. In addition the time series points to a correlation between the index values and blocking

intensities. In other words individual months with stronger pattern index values tend to be blocked for longer time periods.

The above findings are based upon a simplified and condensed representation of the underlying data sets, and indicate that the two-dimensional blocking indicator will permit an effective evaluation of the temporal and spatial correlations. To this end frequency composite maps of the winter APV* blocking index field are calculated on a 6-hourly time resolution for the positive and negative NAO/PNA phases (upper and lower terciles). The different blocking composites are tested against a random climatology distribution with a standard re-sampling (Monte Carlo) test (e.g. Wilks 2005), and a sample of 500 artificial NAO/PNA time series is calculated with the same auto-regression as for the real NAO/PNA indices. Using these time series blocking composites are generated for the lower and upper NAO/PNA terciles and tested for significance on the 98%-level. Note that an individual blocking event can in principal account for both, the positive and negative pattern phase.

For every pattern phase the corresponding 2 pvu isolines (PV2) on different potential temperature levels (from 310 to 325 K at 5 K intervals) are superimposed. To a first approximation, the gradient of these isolines can be re-garded as an indicator of the tropopause gradient and a proxy for the strength of the jet. Notice that the same method in calculating composites has been applied in Scherrer et al. (2006), but they focused solely on the Euro-Atlantic sector.

3.2 North Atlantic blocking: NAO composites

During the positive NAO phase (Fig. 2a) there are three minor blocking frequency maxima. The first is located over Nova Scotia (6%) and the second over Scandinavia (5%). Both locations show small areas with significantly higher frequencies than the blocking climatology (for a display of the climatological frequency values and distributions see Croci-Maspoli et al. 2007). The third centre is located in the North Pacific (9%) and shows no significant differences to the APV* climatology. However, a significantly reduced blocking frequency compared to the APV* climatology can be observed in the North Atlantic region, with a complete absence of blocking during the positive NAO phase. The corresponding PV2 isolines are characterised by a zonally orientated band over North America that crosses the Atlantic and starts to diverge just upstream of the European mainland. An elongated and strong jet south of the decreased blocking frequency is present during the positive NAO phase.

During the negative NAO phase (Fig. 2b), the Atlantic region shows a completely different picture with a signi-

ficantly enhanced blocking frequency over the western North Atlantic (23%, corresponding to more than a dou-bling of the climatological mean value) and no blocking occurrence over central Europe. This behaviour of en-hanced blocking frequency in the negative NAO phase over the northwestern Atlantic has been observed by sev-eral studies (e.g. Pavan and Doblas-Reyes 2000; Stein 2000; Shabbar et al. 2001; Scherrer et al. 2006). It is also reflected in the configuration of the tropopause for the negative NAO phase with a strong ridge-like structure over the central North Atlantic and a more zonal orientation of the PV2 isolines in southern Europe where the jet is weaker.

3.3 North Pacific blocking: PNA composites

Figure 2c, d shows the analogue results for the PNA. The positive PNA phase (Fig. 2c) is characterised by an ab-sence of blocking over the entire North Pacific sector. Minor blocking frequencies are located over western North America (up to 6%) and over the North Atlantic (up to 10%). Notice that these two centres experience signifi-cantly higher frequencies than the climatology. The cor-responding mean tropopause shows the existence of a strong jet over the West Pacific that splits at ~150°W with a ridge-like structure over the American west coast. The relatively weak gradient over western North America agrees well with the local blocking maximum.

The link of the negative PNA phase (Fig. 2d) to the Atlantic blocking distribution remains weak. During the negative PNA phase a pronounced blocking maximum is established in the eastern part of the northern Pacific where blocking frequencies reach up to 20%. This corresponds to approximately ten more blocking days during the winter seasons being experienced in the negative PNA phase in comparison with the full APV* climatology for that region. In addition there is a significantly decreased blocking fre-quency over the western part of North America associated with a broader North American trough. The PV2 isolines during the negative PNA phase are much more dispersed over the date-line region, since the jet is weakened sig-nificantly already upstream east of Japan. Noteworthy are the significant increase (PNA+) and decrease (PNA–) of blocking frequency in the North Atlantic. Similar findings (Dole 1986) attribute the main mechanisms to Rossby wave propagation from the Pacific.

These results suggest that the geographical blocking frequency distribution is significantly different during the opposite NAO/PNA phases and the associated tropopause and jet structures are consistent with the upper-level PV-blocking anomalies. These results provide quantitative information and tentative physical insight on the 'latitude-longitude' blocking distribution and thereby extend previ-

Fig. 2 APV* blocking
frequency (*DJF*) composite
maps for **a** NAO+, **b** NAO−,
c PNA+ and **d** PNA−. Contours
indicate percentage of blockings
during the corresponding
pattern phase. Significance at
98% is shown in *bold black*
(*negative*) and *bold black-white*
(*positive*) contours which are
slightly filtered. Circumpolar
black-white contours indicate
the 2 pvu isolines at different
potential temperature levels
(from 310 to 325 K with 5 K
steps)

4 Blocking influence on regional variability patterns
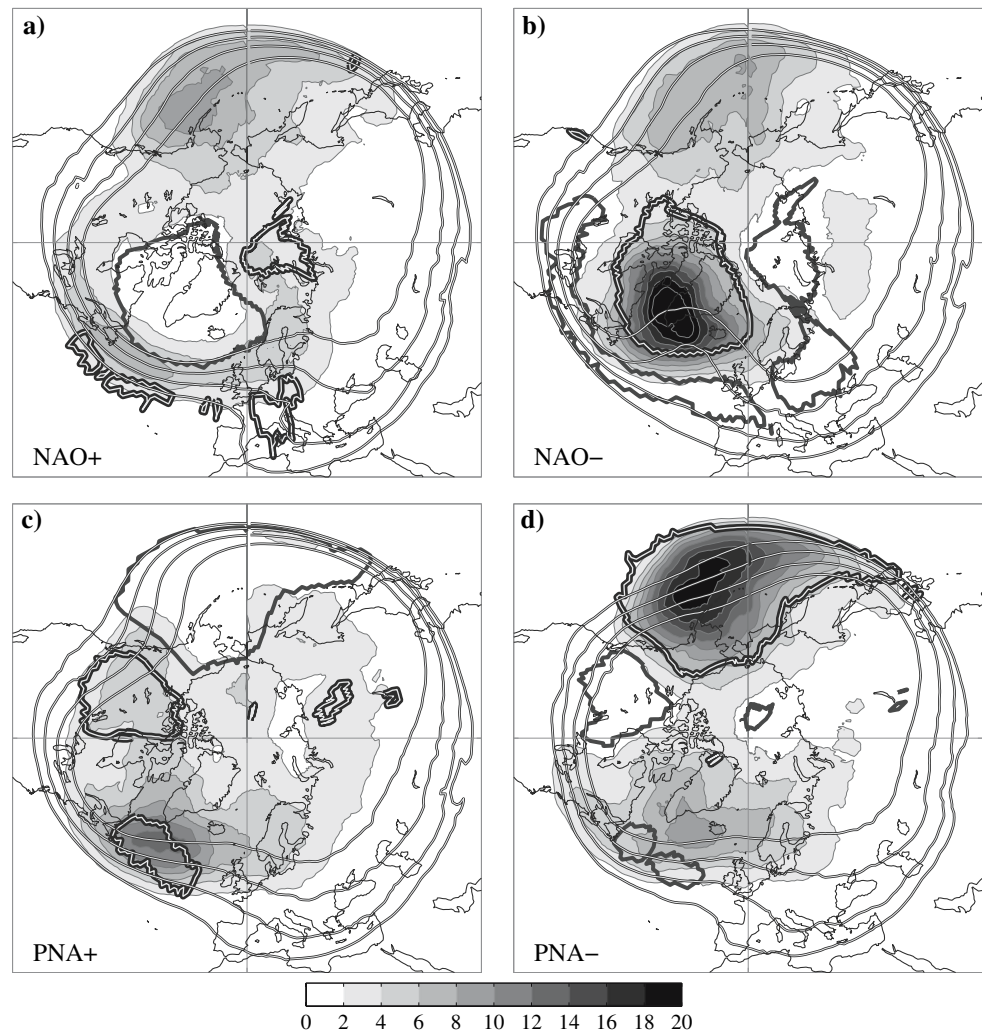
The simple composite analysis in the previous section suggests strong correlations between blocking and the variability patterns, but yields no additional information on the influence of the blocks upon the variability patterns and vice versa. To shed light on the influence of blocks upon the distribution of regional variability patterns we compute EOFs (e.g. Wilks 2005).

The regions of interest are taken as the North Atlantic (80°W–60°E, 30°N–80°N) and North Pacific (120°E–60°W, 30°N–80°N) basin. For the computation we adopt a twofold strategy: (1) EOFs are calculated on a winter monthly basis of the Z500 field for the two regions separately (this set is referred to hereafter as the *original set*), (2) EOFs are calculated of the Z500 as in the first approach but with modified input data that excludes blocked days in the specified region (referred to hereafter as the *modified set*). These missing days are replaced by the corresponding monthly Z500 climatology without blocking days (56% in the North Atlantic and 46% in the North Pacific). The rationale for this replacement is as follows. If, for a particular month, a large fraction of days fall into the blocked category then the modified monthly means constitute a few non-blocking days. This considerably alters the magnitude of the monthly mean and hence the EOF analysis. Indeed months that are entirely blocked would not account for the EOF analysis. To illustrate this point Fig. 3 shows the monthly mean Z500 distribution for the Euro-Atlantic region for January 1963. During this month about 70% of the days are blocked and the strong climatological ridge in the North Atlantic has been replaced by a more zonal flow (Fig. 3b) by the modified Z500 distribution.
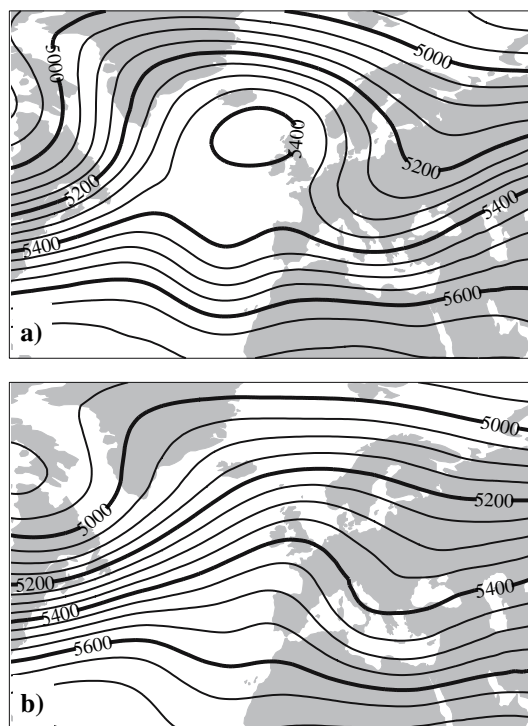
Fig. 3 Illustrative example of the January 1963 Z500 for **a** the monthly mean of all days and **b** the monthly mean without blocking days

4.1 Atlantic EOFs

The first three original EOF patterns over the Atlantic are displayed in Fig. 4a–c. Here, EOF1 (Fig. 4a) resembles the well-known NAO pattern with a meridional dipole structure, and it accounts for 26% of the monthly variability in this region. EOF2 and EOF3 (Fig. 4b,c), accounting for 20 and 14% of the variability, respectively, can be associated respectively with the East Atlantic (EA) pattern (e.g. Wallace and Gutzler 1981) and the mid-latitude anomaly train (MAT) (Massacand and Davies 2001). They are both characterized by a dominant anomaly in the North Atlantic (EA) and over the British Isles (MAT).

The modified EOF patterns (Fig. 4d–f) exhibit a significantly different spatial structure. Here EOF1 is characterized by a tripole-like structure (explained variance 25%) with anomalies of equal sign over the northwest Atlantic and eastern Europe and opposed sign between the British Isles and Scandinavia. The modified EOF2 pattern (22%) resembles a NAO-like distribution and the modified EOF3 (12%) can be classified somewhere between the original EOF2 and EOF3 patterns.

It can be inferred from the above that atmospheric blocking significantly alters the variability patterns over the North Atlantic. Excluding blocking days over the Euro-Atlantic region results in the NAO no longer being the
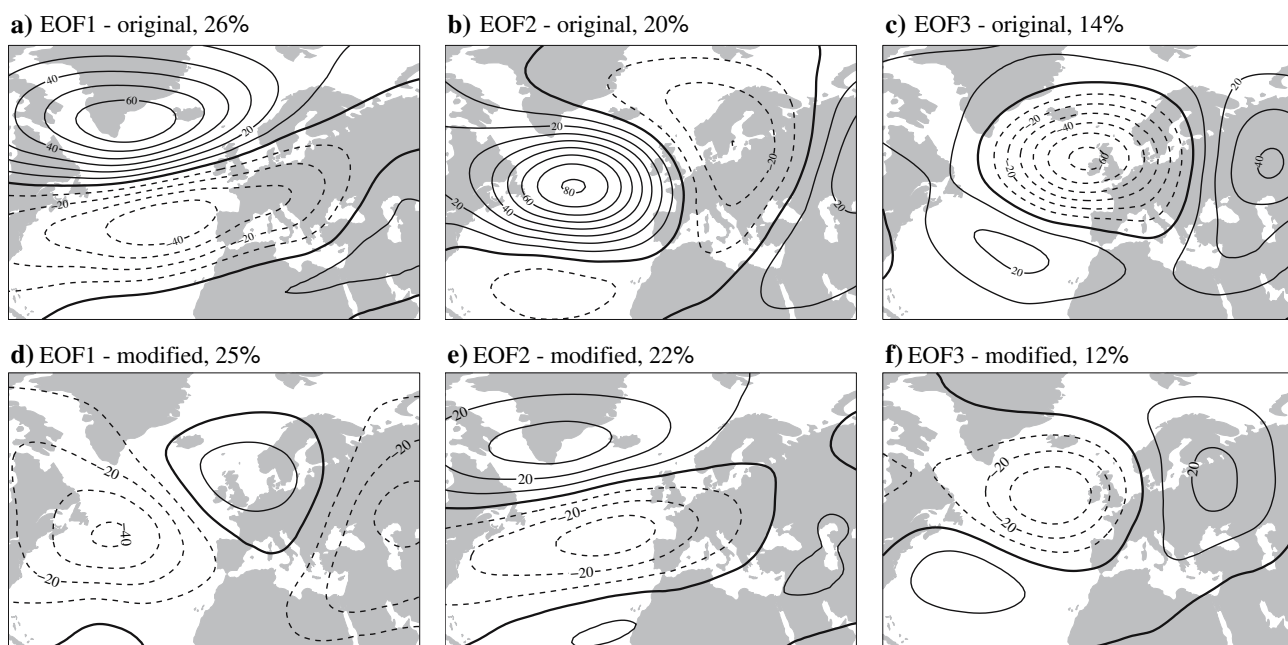
a) EOF1 - original, 26%   **b)** EOF2 - original, 20%   **c)** EOF3 - original, 14%

d) EOF1 - modified, 25%   **e)** EOF2 - modified, 22%   **f)** EOF3 - modified, 12%

Fig. 4 Spatial EOF patterns for the Atlantic region of **a–c** the winter (*DJF*) monthly Z500 climatology and **d–f** the winter monthly climatology without blocking dates (see text for further details).

Shown are deviations (m) from the ERA-40 climatology. *Solid contours* indicate positive anomalies, *dashed contours* negative anomalies and the *zero contour* is indicated in *bold*

dominant pattern of variability but is rather related to the second EOF with 4% less explained variance. The linear correlation (not shown) of the Principal Component (PC) coefficients between the original EOF1 and the modified EOF2 indicates that the temporal agreement is reduced but remains significant ($R = 0.52$). In other words, although the two patterns are very similar with respect to their spatial extent, the temporal correspondence indicates differences and hence modifications to the traditional NAO index. Note that the reduced amplitude of the modified EOFs can at least partly be associated with the substitution of blocking days with the non-blocking climatology.

Furthermore, Scherrer et al. (2006) show a consistent relation between blocking frequency and the EOF3 pattern. In this study we reinforce this finding, since the EOF3 pattern does not explicitly emerge without considering blocking days. It can be hypothesised that the EOF3 pattern indeed does resemble a typical blocking like structure.

4.2 Pacific EOFs

A similar analysis has been performed for the Pacific basin. Figure 5a–c shows the original spatial patterns of EOF1–3. EOF1 resembles the PNA pattern with 26% of the monthly variability (Wallace and Gutzler 1981), and EOF2 (19%) is characterized by a slightly eastward shifted West Pacific (WP) pattern mentioned by, e.g., Barnston and Livezey (1987). It shows both a north–south dipole in the mid-western Pacific and a west–east dipole over the Aleutians and the North American continent. EOF3 explains only 9% of the variance and we merely note that it resembles the

East Pacific (EP) pattern (Barnston and Livezey 1987) but located more to the mid-Pacific.

Compared to the North Atlantic sector, the corresponding modified EOF patterns (Fig. 5e–f) in the North Pacific coincide well with the original patterns. Although the centre of the positive undulation in EOF1 is shifted from western North America (original EOF1) towards the Bering Strait (modified EOF1) it still resembles the structure of the PNA pattern. Considering the temporal evolution of the corresponding PCs yields a statistically significant correlation of 0.72. The pattern of the modified EOF2 is also very similar to the original EOF2 distribution, whereas the modified EOF3 indicates more striking differences but these are not interpreted further due to the associated low value of the explained variability.

It is evident that the results for the North Pacific basin exhibit markedly different behaviour in comparison with those for the North Atlantic where the patterns of variability alter significantly when blockings days are removed from the analysis fields. Hence, it could be argued that the variability in the North Pacific region is influenced to a lesser degree by blocking.

5 Blocking life-cycle studies

In this section the comparative comprehensiveness of the novel blocking climatology is exploited by examining the individual blocking tracks during the different NAO/PNA phases. The dual purpose is to (1) seek novel insight on the characteristics of the tracks and the corresponding genesis
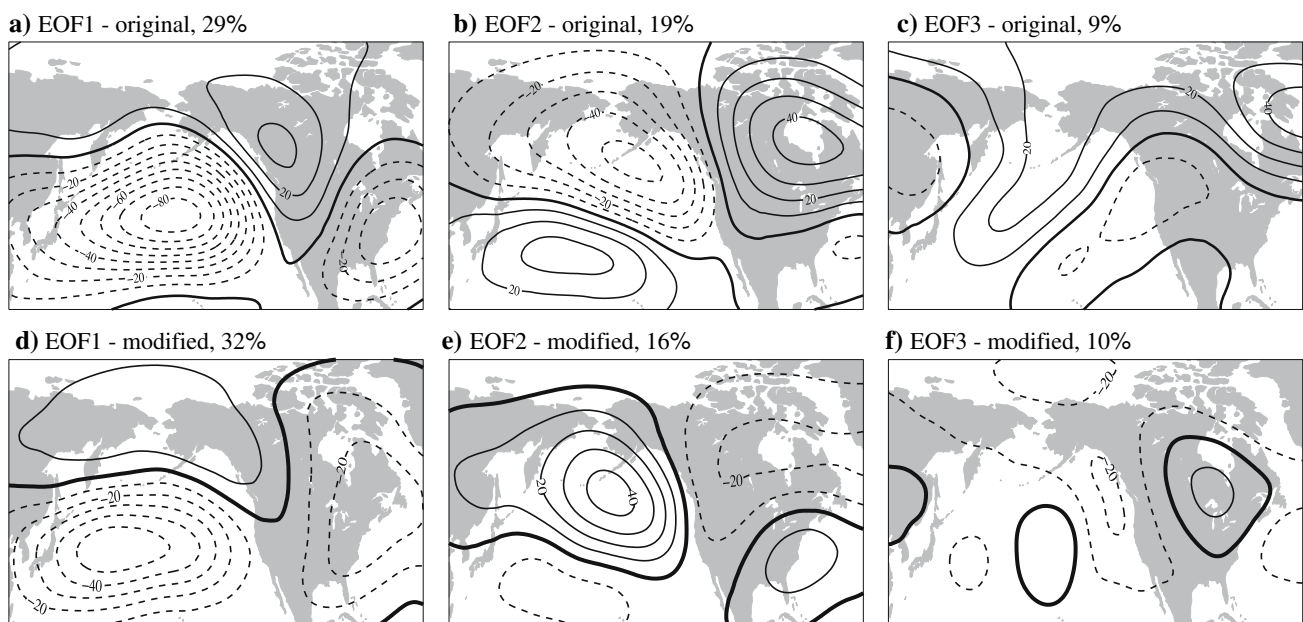

a) EOF1 - original, 29%   **b)** EOF2 - original, 19%   **c)** EOF3 - original, 9%

d) EOF1 - modified, 32%   **e)** EOF2 - modified, 16%   **f)** EOF3 - modified, 10%

Fig. 5 As Fig. 4 but for the Pacific region

and lysis regions during different NAO and PNA phases, and (2) analyse the typical NAO/PNA index evolution during the blocking life-cycle.

To this end the blocking events are subdivided in two ways by (a) their NAO/PNA index value at the time of their genesis and (b) their corresponding ocean basin (NAO – North Atlantic and PNA – North Pacific). Blocking genesis is considered in the North Atlantic (90°W–10°W) and North Pacific (130°W–110°E) basins during the positive, neutral and negative NAO/PNA index phase, respectively. The number of blocking events in each class is summarized in Table 1. Figure 6 displays the individual blocking tracks from genesis (dark dots) to lysis (grey dots) using a colour-scale corresponding to the NAO/PNA index values. Thus, this scheme provides information on the temporal evolution of a pattern's index values during the blocking life-cycle and thereby information on the preferred phase.

5.1 Euro-Atlantic blocking tracks

Figure 6a shows blocking tracks over the North Atlantic with genesis during the negative NAO phase. Blocking genesis occurs in a broad region extending from Newfoundland to the west coast of Greenland and on to between Greenland and Iceland. The blocking tracks are confined predominantly to the neighbourhood of their genesis region, and hence lysis tends to occur in the same area. This result is consistent with the marked blocking frequency maximum in Fig. 2b. The associated NAO values remain negative (blue segments) and only a few tracks reach Scandinavia/Europe.

The direction and index-behaviour of the blocking tracks change fundamentally during the neutral NAO phase (Fig. 6b) with genesis locations spread in a band from Newfoundland towards Iceland. There is a preferred north-eastward movement of the tracks with lysis regions first in the North Atlantic around Iceland with accompanying negative NAO values, and second over the European mainland with positive NAO values (red segments).

Table 1 Number of considered blocking events with genesis in the corresponding index phase. The events are separated into long (≥10 days) and short (<10 days) events. The different pattern phases are divided into three terciles, positive (+), neutral (n) and negative (–)

	Short	Long	Total
NAO+	33	17	50
NAO$_n$	40	18	58
NAO–	34	18	52
PNA+	26	7	33
PNA$_n$	37	20	57
PNA–	45	37	82

The north-eastward movement is even more significant for blocks starting in the positive NAO phase (Fig. 6c). It is evident that during the positive NAO phase blocks develop over a strictly confined area of Newfoundland and the western North Atlantic ocean. Compared to the NAO pattern (cf. Fig. 4a), this genesis region is located between the positive and negative centres of the NAO pattern itself and corresponds to the local frequency maximum evident in Fig. 2a. Most of the tracks span the entire North Atlantic and lysis is favoured over north-western Europe. During some of these blocking evolutions the NAO index remains mainly in the positive NAO tercile especially for the more southern tracks. However, a significant amount of blocking lysis ends in the neutral or even negative NAO tercile.

In summary, although the mean propagation of the blocks between genesis and lysis is towards the northeast for all pattern phases, a clear signal for individual retrogressing life-cycles can be observed, especially during the mature phase of the block. A preference for retrogression is observed during the negative NAO phase. It is conceivable that this distinctive behaviour over the Atlantic during the negative NAO phase might be associated with the slow westward movement of low-frequency (20-day period) planetary-scale waves (Doblas-Reyes et al. 2001).

5.2 North Pacific blocking tracks

The blocking tracks in the Pacific sector during the different phases of the PNA exhibit some notable differences. For instance, only few blocks start at either the Asian east coast or the North American west coast in the positive PNA phase (Fig. 6f). The direction of the tracks is not very coherent and hence the lysis region is not well confined. The number of events increases during the PNA$_n$ phase (Fig. 6e) where especially mid-Pacific tracks tend to develop into a negative PNA. This characteristic is even more evident for blocks that start in the negative PNA phase (Fig. 6d), and these basically remain in the negative PNA phase throughout their evolution.

5.3 Evolution of variability patterns during blocking life-cycles

The previous findings suggest some interesting dynamical cause–effect relationships between the phase of the index and blocking. To examine this relationship further the mean evolution of the pattern index values throughout the life-cycle of the blocks in each of the considered classes (cf. Table 1) is examined and compared with a climatological/randomized NAO/PNA index evolution.

To this end the mean NAO/PNA index value of the individual blocking tracks in each class (cf. Table 1) are calculated at every 6-hourly time step starting from genesis
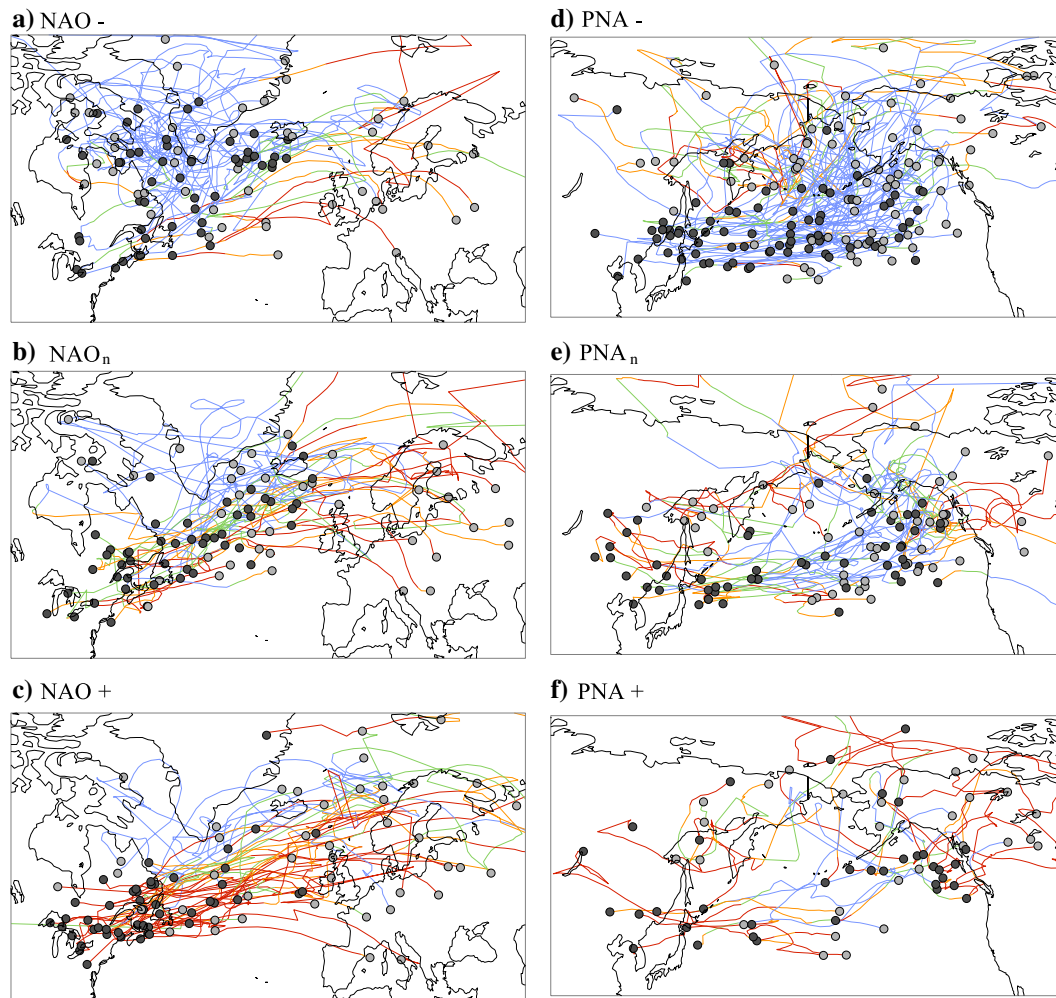
Fig. 6 Distribution of winter APV* blocking genesis (*dark dots*) and lysis (*light dots*) with the corresponding track lines during **a** NAO–, **b** NAO$_n$, **c** NAO+ in the Atlantic region and **d** PNA–, **e** PNA$_n$, and **f** PNA+ in the Pacific region. Only tracks are displayed with genesis in the corresponding index phase whereas lysis does not have to be in this region. The colour scaling indicates four partitions of the index values, namely; *blue* NAO < –0.34, PNA < –0.39; *green*: NAO < 0, PNA < 0; *orange* NAO > 0, PNA > 0; *red* NAO > 0.52, PNA > 0.52

and ending after the first 5 days (Fig. 7). Also the same procedure is performed by starting at blocking lysis and incorporating the preceding 5 days. Analysis is also performed with a further subdivision into long-lasting (>10 days) and short-lasting (5–10 days) blocking events. For the following discussion note that the number of blocking events varies considerably for the Pacific, where significantly more than 50% of the blocking events are established during the negative PNA phase (82) in comparison with the positive phase (33). In comparison recall that blocking genesis occurs equally often in the three NAO phases (cf. Fig. 6). In addition a randomized sample (1,000 re-samplings) of daily NAO/PNA evolutions starting in the different tercile boundaries is calculated, and the 95% confidence interval is used for significance testing.

The randomized NAO/PNA index evolution (Fig. 7, grey shading) exhibits within the first 4–5 days a nonlinear

increase (decrease) from mean NAO/PNA starting values of around –1 (1) towards values approaching 0. This can be interpreted as the typical decay time-scale of the corresponding variability patterns. Hence, assuming a similar time-scale for the pattern growth as for the decay a full NAO life-cycle would last about 9 days. This corresponds well to the proposed typical NAO life-times of 7.4–9.2 days by Feldstein (2000). The randomized neutral NAO/PNA patterns remain neutral (Fig. 7, middle row).

The index evolution for blocking events that start in the negative NAO/PNA phase (Fig. 7a, d) show that the mean NAO/PNA value remains almost constant throughout the entire genesis phase of the block, and are significantly below the randomized mean. This indicates a slower than normal relaxation of the variability pattern during a blocking situation. The blocking-mean index continues to be significantly below (i.e. more extreme) the randomized

Fig. 7 Evolution of the **a–c** NAO and **d–f** PNA index values for blocking events with onset in different pattern phases (index tercile boundaries indicated by the *horizontal thin lines*). In *red* only short (<10 days), in *blue* only long (≥10 days) and in *black* the total number of blocking events is considered. The mean randomized index evolution (1,000 re-samplings) is indicated in *bold grey* and the *grey shading* indicates the corresponding 95% confidence interval. Significant different index evolutions from the randomized sample are indicated in *bold*. Note that the abscissa is split in a genesis (*left*) and lysis (*right*) phase
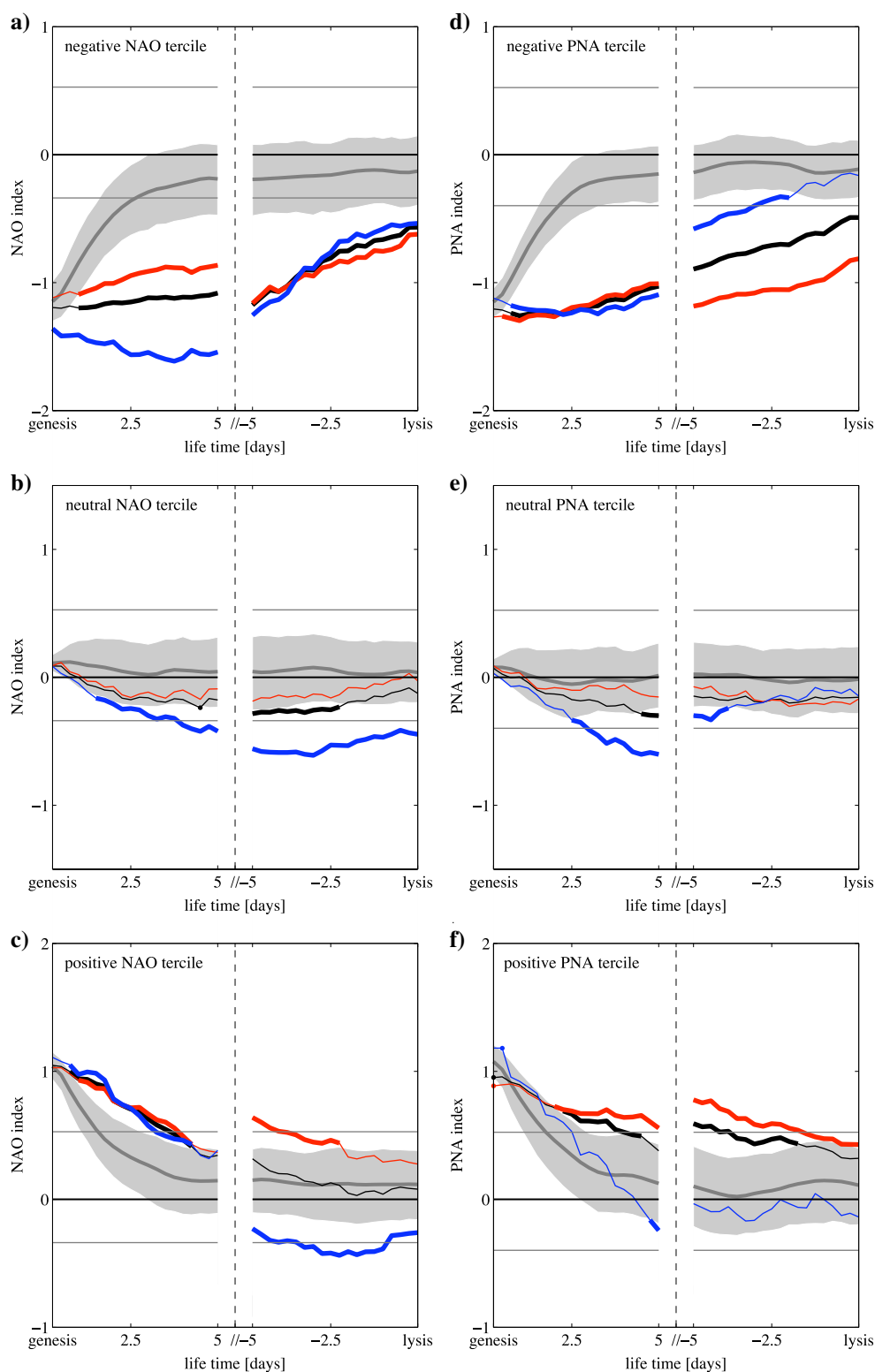
mean throughout the entire blocking life-time through to lysis. It is interesting to note the different behaviour in the North Atlantic and Pacific. In the Pacific, the blocked-sample for the PNA mean develops similarly in the genesis phase independent of the total life-time of the blocks. Yet

in the Atlantic a clear separation is evident, with long-lasting blocks (duration of more than 10 days) having a larger negative NAO index mean during genesis, than the shorter-lived block sample. In particular, the long-lasting blocks develop on significantly more intense negative NAO

background flows. For the lysis phases this behaviour is reversed, such that the decay of the block-NAO mean evolves independently of the total life-time, unlike for the block-PNA mean, where the negative PNA variability pattern decays markedly slower for long-lived blocks.

For blocks starting in the neutral phases (Fig. 7b, e) there is the tendency for the index to remain neutral or slightly negative throughout the genesis and the lysis phase. In the presence of long-lasting blocks the flow even exhibits a phase change from neutral towards negative NAO/PNA values. Since this phase change only occurs after the blocks have existed for a few days, it is viable to assume that the existence of the long-lasting blocks exert an effect on the phase of the variability pattern.

In the Atlantic this influence of the long-lasting blocks on the large-scale flow is even more evident (Fig. 7c). Here, the initial flow state at genesis is in the positive NAO phase, but experiences a marked phase transition into the negative NAO phase by the time of blocking lysis. This behaviour is also apparent, though not significant in the Pacific (Fig. 7f), but is not observed for the shorter-lasting blocks, indicating that these systems might not be strong or persistent enough to be associated with a large-scale phase transition of the flow.

Reconsideration of Fig. 6 prompts a further interpretation. In the Atlantic many blocks that still reside in a NAO+ state at lysis are located over central Europe, where their existence provides dynamical reinforcement of the NAO+ phase by locally lifting the tropopause and enhancing the existing jet towards their north. The long-lived blocks, that initiate a phase change on the other hand, are located much further towards the north, thereby weakening the Icelandic pole of the NAO pattern and the accompanying jet stream. An analogous interpretation is possible for the Pacific region, where the blocking tracks that end near the negative lobe of the PNA pattern in Fig. 5a support the negative PNA phase and vice versa for the more northerly tracks that end over the American continent and within the positive (in Fig. 5a) centre of the pattern.

It is also noteworthy that the large-scale flow pattern that is prone to blocking genesis in the Atlantic is linked to a stronger than normal positive NAO phase (Fig. 6a), stronger than normal negative NAO phase for the genesis of long-lasting blocks (Fig. 6c), and a stronger than normal negative PNA phase in the Pacific (Fig. 6f).

6 Summary and further remarks

In this study the occurrence and character of atmospheric blocks has been examined in combination with the concurrent temporal evolution of the standard NAO and PNA indices. The derived results provide novel quantitative insight on the spatial and temporal linkage of blocks to the phases of the NAO and PNA patterns, and in particular point to the importance of atmospheric blocking to the modulation and evolution of NAO and PNA variability.

Here, as a prelude to commenting on some of the dynamical and forecasting implications of the study, we pinpoint four pivotal features of the study. First a clear temporal co-variability has been found between the NAO (PNA) index values and blocking frequency and duration in the Atlantic (Pacific) basins (Fig. 1). Recall that the basins themselves are the seat of the major climatological centers of blocking activity in the Northern Hemisphere.

Second composite maps (Fig. 2) of blocking for the opposing PNA/NAO phases derived from a novel two-dimensional blocking climatology (Croci-Maspoli et al. 2007) provide a detailed spatial description of the co-variability. In particular, it is shown that the northwest Atlantic (central North Pacific) exhibits significantly higher blocking frequencies during the negative NAO (PNA) phase (>100% increase compared to the local climatological values that translates to ~10 days more blocking per season). The corresponding positive index phase is characterised by the near absence of blocking in these same regions. Moreover, the two-dimensional representation of blocking composites provides detailed information on the precise location and frequency of blocks and thereby both refines and extends extant studies that have focussed predominantly on the longitudinal blocking distribution (e.g. Pavan et al. 2000; Shabbar et al. 2001). In harmony with the results presented herein other recent two-dimensional blocking representations of NAO-only composites (Barriopedro et al. 2006; Scherrer et al. 2006) also point to significantly higher blocking frequencies over the western/central North Atlantic during the negative NAO phase and over Northern Europe during the positive phase.

Third, a simple but illuminating statistical approach is employed that helps identify atmospheric blocking as a major contributor to NAO and PNA variability. In essence the approach entails compiling two different regional EOF analyses of Z500. One incorporates all winter days (the original set) and a second (the modified set) excludes blocked days that occur in the selected region (Figs. 4, 5). For the Atlantic the results suggest that Euro-Atlantic blocks exert a considerable influence upon the in situ EOF patterns, such that the NAO-like EOF pattern of the modified set is no longer the lead pattern. For the Pacific the changes are not so dramatic with the PNA-like pattern of the modified set remaining the lead EOF but with a marked change in the shape and position of the variability centres.

Fourth, it is found that the realized blocking genesis and lysis regions during the opposing phases of the NAO/PNA are strikingly different (Fig. 6). In the Atlantic blocks

spawned in the positive NAO phase have a confined genesis region around Nova Scotia and a distinctively separate lysis region over Northern Europe. This is in contrast to blocks spawned in the positive phase, which show a diffuse genesis region encompassing a comparatively large area over the Bering Strait and lysis occurs in the same region. In the North Pacific the number of genesis events differs notably between the positive and negative PNA phases with formation favoured during the negative PNA phase (87 events) compared to the positive PNA phase (33 events). Also the variations in genesis and lysis locations are accompanied by marked variations in blocking track direction, speed and length.

We now turn to consider more dynamically-related features related to the blocking life-cycle itself. Our analysis indicates that the characteristics of the life-cycle are related to the temporal evolution and phase changes of the concomitant variability patterns (Fig. 7). Some of the related inferences are that blocks: (1) sustain the *negative* NAO/PNA phase from genesis to lysis; (2) increase the life-time of the negative phase of the patterns and extend the decay time scale of the variability patterns; (3) can, dependent upon their location, help sustain the *positive* NAO/PNA phase; (4) can instigate a *phase transition* from a neutral or even positive pattern phase into the negative phase, especially for long-lasting blocks and this is most evident over the North Atlantic.

In the context of point (4) we note that block location at lysis relative to the variability centre plays a crucial role in triggering a phase change, and that an equivalent, albeit non-significant, interrelation is found for long-lived Pacific blocks and PNA positive-to-negative phase shifts. Also in connection with point (4) a complementary calculation to that in Fig. 7 can be derived but for all the NAO/PNA phase transitions (with positive to negative phase within 10 days) and associated with the co-occurrence of blocks. The result indicates that 56% of the NAO transitions in the North Atlantic are associated with atmospheric blockings (36% for PNA/North Pacific), and this strongly supports the earlier conclusions drawn from Fig. 7. By way of a caveat we note that not all blocks trigger a NAO phase transition, and not all of the NAO variability results from the occurrence of blocking.

Some characteristics of blocking life-cycles are similar in the North Atlantic and the Pacific area. Nevertheless, our results suggest that different factors contribute to the local variability in the Pacific and North Atlantic. First consider the relative number of block genesis in the North Pacific during opposing phases of the PNA. The difference is striking and suggests that the phase of the background PNA field can influence block formation with the negative PNA phase favouring and the positive phase suppressing block onset. More specifically most blocks develop during

significantly intensified negative PNA states. In this context it is pertinent to note that PNA variability has itself been linked to the equatorial SST and strong El Nino / La Nina events (Horel and Wallace 1981). Likewise tropical sources have been invoked to account for North Pacific blocks (e.g. Renwick and Wallace 1996).

In the North Atlantic the results indicate that the conditions that favour the establishment of North Atlantic blocks include an intense NAO base state during genesis. A distinct difference during the opposing phases is the clear geographical separation of the genesis points. It was shown that in the Euro-Atlantic sector blocks significantly contribute to the establishment of – primarily – the negative NAO phase, owing to the location of the blocking tracks. A corollary is that the reverse phase change to positive index values requires alternative explanation(s). In this context, we note that Benedict et al. (2004) describe the positive NAO phase as the remnant of two consecutive anticyclonic wave breakings at the west coast of North America and the subtropical North Atlantic and there is corroborative evidence for such a description (Feldstein 2003; Franzke et al. 2004).

In summary, this study's results emphasize the strong relationships between atmospheric blocking and the dominant climate modes in both the Atlantic and Pacific basin. Furthermore a systematic analysis of the individual blocking tracks points to the existence of a causal relationship in the North Atlantic with a space-time link between the essentially statistical pattern of climate variability and the dynamically distinct entity of an atmospheric block.

A possible dynamical explanation for this linkage was hinted at in the introduction. It is that the previously noted synoptic-scale wave-breaking precedes both the establishment of the NAO and the block. Our results lend further support to this close relationship. In addition, consistent with the results of Feldstein (2002), we find less of an influence on the PNA pattern.

Finally, we note that the predilection for atmospheric blocking to establish negative index phases has implications for medium range, seasonal and climate predictions and for the interpretation of Global Climate Model (GCM) output. For the medium range the challenge would be to ensure that a blocking event is adequately replicated so as to herald the onset of a phase change. Likewise for seasonal and climate predictions there are implications related to the systematic underestimation of blocking frequency (e.g. Tibaldi and Molteni 1990; Doblas-Reyes et al. 1998) especially in low-resolution GCMs and ensemble predictions (e.g. Mauritsen and Källen 2004). In a similar vein models that relegate the NAO/PNA signal to the second or third EOF might also be indicative of underestimating the correct blocking frequency. In this context, we note that

recent GCM simulations (Ringer et al. 2006) show much more realistic variability patterns and an improved representation of blocking, but there remains an under- and overestimation of blocking frequency and a mis-representation of the leading large-scale variability patterns.

References

Barnston AG, Livezey RE (1987) Classification, seasonality and persistence of low-frequency atmospheric circulation patterns. Mon Weather Rev 115:1083–1126

Barriopedro D, Garcia-Herrera R, Lupo AR, Hernandez A (2006) A climatology of northern hemispheric blocking. J Clim 19:1042–1063

Benedict JJ, Lee S, Feldstein SB (2004) Synoptic view of the North Atlantic oscillation. J Atmos Sci 61:121–144

Croci-Maspoli M, Schwierz C, Davies HC (2007) A multi-faceted climatology of atmospheric blocking and its recent linear trend. J Clim 20:633–649

Doblas-Reyes FJ, Deque M, Valero F, Stephenson DB (1998) North Atlantic wintertime intraseasonal variability and its sensitivity to GCM horizontal resolution. Tellus 50:573–595

Doblas-Reyes FJ, Pastor MA, Casado MJ, Deque M (2001) Wintertime westward-traveling planetary-scale perturbations over the Euro-Atlantic region. Clim Dyn 17:811–824

Dole RM (1986) The life-cycles of persistent anomalies and blocking over the North-Pacific. Adv Geophys 29:31–69

Dole RM, Gordon ND (1983) Persistent anomalies of the extratropical northern hemisphere wintertime circulation—geographical-distribution and regional persistence characteristics. Mon Weather Rev 111:1567–1586

Ertel H (1942) Ein neuer hydrodynamischer Wirbelansatz. Meteorol Z 59:277–281

Feldstein SB (2000) The timescale, power spectra, and climate noise properties of teleconnection patterns. J Clim 13:4430–4440

Feldstein SB (2002) Fundamental mechanisms of the growth and decay of the PNA teleconnection pattern. Q J R Meteorol Soc 128:775–796

Feldstein SB (2003) The dynamics of NAO teleconnection pattern growth and decay. Q J R Meteorol Soc 129:901–924

Franzke C, Lee S, Feldstein SB (2004) Is the North Atlantic oscillation a breaking wave? J Atmos. Sci 61:145–160

Horel JD, Wallace JM (1981) Planetary-scale atmospheric phenomena associated with the southern oscillation. Mon Weather Rev 109:813–829

Huang F, Zhou FX, Qian XD (2002) Interannual and decadal variability of the North Pacific blocking and its relationship to SST, teleconnection and storm tracks. Adv Atmos Sci 19:807–819

Lupo AR, Smith PJ (1995) Climatological features of blocking anticyclones in the northern-hemisphere. Tellus 47:439–456

Massacand AC, Davies HC (2001) Interannual variability of European winter weather: the potential vorticity insight. Atmos Sci Lett 2:52–60

Mauritsen T, Källen E (2004) Blocking prediction in an ensemble forecasting system. Tellus 56:218–228

Pavan V, Doblas-Reyes FJ (2000) Multi-model seasonal hindcasts over the Euro-Atlantic: skill scores and dynamic features. Clim Dyn 16:611–625

Pavan V, Tibaldi S, Brankovic C (2000) Seasonal prediction of blocking frequency: results from winter ensemble experiments. Q J R Meteorol Soc 126:2125–2142

Pelly JL, Hoskins BJ (2003) A new perspective on blocking. J Atmos Sci 60:743–755

Renwick JA, Wallace JM (1996) Relationships between North Pacific wintertime blocking, El Nino, and the PNA pattern. Mon Weather Rev 124:2071–2076

Ringer MA, Martin GM, Greeves CZ, Hinton TJ, James PM, Pope VD, Scaife AA, Stratton RA, Inness PM, Slingo JM, Yang GY (2006) The physical properties of the atmosphere in the new Hadley Centre Global Environmental Model (HadGEM1). Part II: Aspects of variability and regional climate. J Clim 19:1302–1326

Sausen R, König W, Sielmann F (1995) Analysis of blocking events from observations and ECHAM model simulations. Tellus 47:421–438

Scherrer SC, Croci-Maspoli M, Schwierz C, Appenzeller C (2006) Two-dimensional indices of atmospheric blocking and their statistical relationship with winter climate patterns in the Euro-Atlantic region. Int J Climatol 26:233–249

Schwierz C, Croci-Maspoli M, Davies HC (2004) Perspicacious indicators of atmospheric blocking. Geophys. Res Lett 31:Art. No. L06125

Shabbar A, Huang JP, Higuchi K (2001) The relationship between the wintertime North Atlantic oscillation and blocking episodes in the North Atlantic. Int J Climatol 21:355–369

Stein O (2000) The variability of Atlantic-European blocking as derived from long SLP time series. Tellus 52:225–236

Straus DM, Shukla J (2002) Does ENSO force the PNA?. J Clim 15:2340–2358

Tibaldi S, Molteni F (1990) On the operational predictability of blocking. Tellus 42A:343–365

Uppala SM, Kallberg PW, Simmons AJ, Andrae U, Bechtold VD, Fiorino M, Gibson JK, Haseler J, Hernandez A, Kelly GA, Li X, Onogi K, Saarinen S, Sokka N, Allan RP, Andersson E, Arpe K, Balmaseda MA, Beljaars ACM, Van De Berg L, Bidlot J, Bormann N, Caires S, Chevallier F, Dethof A, Dragosavac M, Fisher M, Fuentes M, Hagemann S, Holm E, Hoskins BJ, Isaksen L, Janssen P, Jenne R, McNally AP, Mahfouf JF, Morcrette JJ, Rayner NA, Saunders RW, Simon P, Sterl A, Trenberth KE, Untch A, Vasiljevic D, Viterbo P, Woollen J (2005) The ERA-40 re-analysis. Q J R Meteorol Soc 131:2961–3012

Wallace JM, Gutzler DS (1981) Teleconnections in the geopotential height field during the northern hemisphere winter. Mon Weather Rev 109:784–812

Wilks DS (2005) Statistical methods in the atmospheric sciences, vol 91. Academic Press, San Diego, USA